The X-Ray Atomic and Molecular Spectroscopy Program at the Advanced Light Source

D. W. Lindle, O. Hemmers, P. Glans, D. L. Hansen, H. Wang, and S. B. Whitfield
Department of Chemistry, University of Nevada,
Las Vegas, NV 89154-4003, USA

R. Wehlitz, J. C. Levin, and I. A. Sellin
Department of Physics and Astronomy, University of Tennessee,
Knoxville, TN 37996-1200, USA

R. C. C. Perera
Advanced Light Source, Lawrence Berkeley National Laboratory,
Berkeley, CA 94720, USA

Abstract: The X-ray Atomic and Molecular Spectroscopy program at the Advanced Light Source is a new research collaboration conceived to take advantage of the latest generation of synchrotron-radiation facilities in pursuit of fundamental investigations of atomic and molecular interactions with x-rays. The research team represented in this program has designed specialized equipment to deliver and use high-resolution x-ray beams to perform electron, ion, and x-ray spectroscopies on atoms and molecules. An overview of the program is presented, and one example of some of the exciting new results obtained thus far is included.

1. Introduction

The X-ray Atomic and Molecular Spectroscopy (XAMS) program at the Advanced Light Source (ALS) is a collaborative effort representing a large team of researchers [1]. The team is interested in using highly monochromatic x-ray beams in fundamental investigations of the physical and chemical phenomena of primary importance to the understanding of core-level processes in atoms and molecules. Over the past two years, state-of-the-art instrumentation for electron spectroscopy, ion spectroscopy, and x-ray-emission spectroscopy has been constructed in order to enhance capabilities within the U.S. for the study of atomic and molecular core-level phenomena. Furthermore, the team has preferred access to the brightest x-ray source in the world, the ALS at the Lawrence Berkeley National Laboratory. Preferred access is in the form of a beamline, a device which delivers focussed and monochromatic x-ray beams in the 1-6 keV photon-energy range to experimenters, and that is built for and dedicated to the team's research program.

The scientific interests of the XAMS program focus on phenomena that are most readily studied via x-ray interactions with atoms and molecules, such as x-ray resonant-Raman effects, non-electric-dipole effects on photoionization, and polarization-sensitive x-ray emission. Overall, this program seeks to undertake a new broad-based effort in this area of research, both because of intrinsic interest in a more detailed understanding of atomic and molecular x-ray interactions, and because results in this area have been relatively scarce due to the paucity of x-ray beamtime and equipment available for their pursuit.

The remainder of this paper is organized as follows. First, a general description of the scientific interests encompassed by the XAMS program is given in Sec. 2. Second, experimental facilities available to the team, both an ALS x-ray beamline and individual systems capable of different types of spectroscopy, are described briefly in Sec. 3. Finally, an example of initial results obtained by the team, specifically on non-dipolar angular distributions in neon valence photoemission, are discussed in Sec. 4.

2. Scientific Program

The XAMS program, although designed for versatility in its experimental pursuits, has six designated research-focus areas, selected both because of their scientific interest and because of a general scarcity of previous results. One focus area for this program is a first look at transient atomic species (e.g., atomic sulfur) and free radicals (e.g., HS) in the deep-core-level region. To our knowledge, no such experiments have ever been done. A second focus

area is core-level resonant-Raman spectroscopy, both radiative (i.e., x-ray emission) and non-radiative (i.e., resonant-Auger emission). Earlier studies [2-9] have illustrated both the promise of this technique as well as the extreme difficulty of the measurements due to the simultaneous needs of high x-ray flux and high energy resolution. The third focus area is molecular photoionization and photofragmentation dynamics [10,11] following deep-core-level absorption. In order to unravel the multitude of possible decay paths (radiative, non-radiative, and fragmentation), ion, electron, and x-ray-emission spectroscopies are all needed, in coincidence when feasible.

The fourth focus area for the XAMS program centers on the effects of non-electric-dipole processes on photoionization, most readily revealed in photoelectron angular distributions. Recent work [12] has demonstrated the accessibility of this phenomenon with the advent of high-brightness synchrotron-radiation sources. Aside from their intrinsic interest, it is important to determine the extent of these effects on measurements in a variety of fields that rely on the common technique of photoelectron spectroscopy. A fifth focus area is polarized x-ray-emission spectroscopy of molecules. Previous results [13] with a dedicated beamline and endstation at the National Synchrotron Light Source showed the great promise of this technique for structural and dynamical studies of molecules. Finally, the sixth focus area is in detailed studies of electron-correlation phenomena. This area is exemplified by single-photon double photoionization of helium. A proper description of this phenomenon, for which increasingly precise measurements are now being performed, requires solution of the Coulomb three-body problem with extremely accurate treatment of electron-electron interactions [14-16]. In the first two years of this new program, preliminary results in 5 of the 6 focus areas have been obtained.

3.   Experimental Program

In order to carry out this scientific program, ready access to a high-resolution, high-brightness x-ray source is required. To attain this access, members of the XAMS team designed and built an x-ray beamline at the ALS for x-ray-spectroscopy applications. This device, designated ALS beamline (BL) 9.3.1 [17], is built around a mechanically precise double-crystal monochromator capable of yielding high photon-energy resolution $E/\Delta E \approx 7,000$ in the 1-6 keV region. The beamline's optical design, with a collimating pre-mirror and a focussing post-mirror, preserves the high brightness of the ALS source, providing a well-focussed x-ray beam (0.2×0.4 mm) to the experiment. Because of these characteristics, BL 9.3.1 delivers brightness [photons/(s mm^2 mrad ΔE)] an order-of-magnitude higher than any other similar

beamline in its energy range, while maintaining energy resolution and flux equal to other lines. Also notable is that BL 9.3.1 is one of only two beamlines at the ALS (the other operates in the 20-300 eV range) to have a significant amount of beamtime dedicated to atomic and molecular research; the allocation of beamtime at BL 9.3.1 accounts for about 60% of the beamtime at the ALS set aside for this community.

Along with a reliable source of x-rays, versatile, state-of-the-art instruments for x-ray-spectroscopic measurements are needed to carry out this research program. At present, five instruments are part of this program: (1) a high-resolution angle-resolved electrostatic electron spectrometer, (2) a gas cell for photoabsorption measurements, (3) a polarization- and angle-resolved x-ray-emission spectrometer, (4) angle-resolved time-of-flight (TOF) electron spectrometers, and (5) an ion-TOF spectrometer. Because the preliminary results discussed below were obtained with the electron-TOF apparatus, the remainder of this section will focus on its characteristics.

The electron-TOF system is a stand-alone apparatus that presently has three operational analyzers (a fourth will be available by late 1996). These analyzers are based on a new design that includes cylindrical focussing to preserve accurate timing resolution while dramatically improving the collection efficiency for highly retarded electrons. For example, in measurements with this apparatus, electrons with 1-keV initial kinetic energy have been retarded to 50-eV final kinetic energy with no loss in throughput. Because electron-TOF energy resolution is directly proportional to the final kinetic energies of electrons, this new design allows efficient electron spectroscopy with energy resolution comparable to or better than most conventional electrostatic analyzers. To maintain ultimate timing resolution for this new generation of TOF analyzer, significant care was taken in the design of the microchannel-plate detectors and impedance-matched conical anodes. Likewise, the best commercially available electronic modules were obtained, allowing simultaneous operation of up to four analyzers with 8192 data points per analyzer and a fixed downtime of only 0.8 μs per event for each analyzer. As a result this system provides timing and data-collection capabilities that meet or exceed those of any other electron-TOF system in use with synchrotron radiation. Further details of the new apparatus will be presented in a forthcoming publication. A more-detailed discussion of a similar apparatus is given by Becker et al. [18].

The electron-TOF analyzers are mounted in a vacuum chamber which can be rotated about the x-ray beam. The chamber includes two additional analyzer mounting ports 54.7° out of the plane perpendicular to the x-ray-beam direction, a geometry which permits direct and sensitive measurement of non-dipolar angular-distribution parameters for photoelectrons. To see how non-electric-dipole interactions can affect photoelectron angular distri-

butions, it is helpful to first look at the consequences of the well-known dipole approximation. The electric-dipole ($E1$) approximation for photon interactions ($\exp(ikr) \approx 1$ [19] leads to the following expression for the differential photoionization cross section [20]:

$$\frac{d\sigma}{d\Omega} = \frac{\sigma}{4\pi}\left[1 + \frac{\beta}{2}(3\cos^2\theta - 1)\right] \tag{1}$$

which describes the angular distribution of photoelectrons from a randomly oriented sample created by 100% linearly polarized light. Here, σ is the partial photoionization cross section, and the angle θ is defined in Fig. 1. The parameter β completely describes the angular distribution of photoelectrons, within the dipole approximation. In this approximation, all higher-order interactions, such as electric-quadrupole ($E2$) and magnetic-dipole ($M1$), are neglected. Over the past two decades, the dipole approximation has facilitated a basic understanding of the photoionization process in atoms and molecules [21], as well as the application of photoelectron spectroscopy to a wide variety of condensed-phase systems.

4. Electric-Quadrupole and Magnetic-Dipole Effects on Neon Valence Photoemission

The first hint of low-photon-energy (i.e., ≤ 5 keV) deviations from the dipole approximation was provided by Krause [22] in measurements using unpolarized x-rays [23]. A small deviation from the expected dipolar angular distribution at photon energies between 1 and 2 keV was observed and attributed to the influence of $E2$ and $M1$ interactions, which are included in the approximation $\exp(ikr) \approx 1 + ikr$. These higher-order corrections to the dipole approximation lead to so-called *non-dipole* effects, such as retardation (photon momentum transfer), in the angular distributions of photoelectrons, and can be described by [24]

$$\frac{d\sigma}{d\Omega} = \frac{\sigma}{4\pi}\left[1 + \frac{\beta}{2}(3\cos^2\theta - 1)\right]$$
$$+ \frac{\sigma}{4\pi}\left[(\delta + \gamma\cos^2\theta)\sin\theta\cos\phi\right] \tag{2}$$

for 100% linearly polarized light. The angle ϕ is defined in Fig. 1, and γ and δ are non-dipole angular-distribution parameters. The initial experiments [22,25] motivated theoretical work [26,27], and recent publications
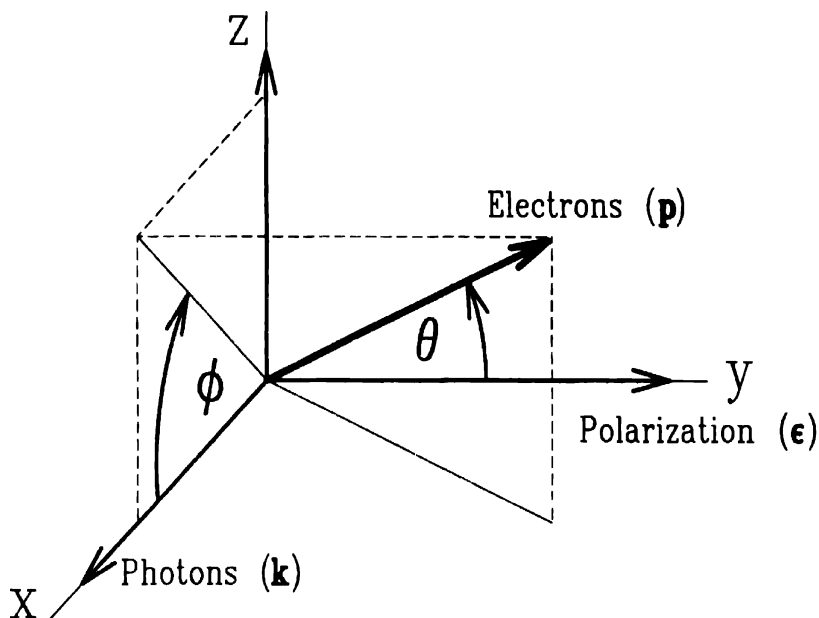
Fig. 1. Geometry applicable to photoelectron angular-distribution measurements us-
ing polarized light. θ is the polar angle between the photon polarization vector ε and the mo-
mentum vector *p* of the photoelectron. φ is the azimuthal angle defined by the photon
propagation vector *k* and the projection of *p* into the x-z-plane.

[24,28,29] include quantitative predictions for a variety of atomic subshells.
Very recently, more extensive measurements [12,30], focussing on noble-gas
core levels (Ar *K* and Kr *L*) and photon energies above 2 keV, have begun to
investigate non-dipole effects in photoelectron angular distributions in more
detail.

In contrast, the present experiment concentrates on the Ne 2*s* and 2*p*
valence subshells at relatively low photon energies (≤ 1.2 keV). Non-dipole
effects are observed to be significant in this energy regime and measurable at
energies as low as 0.25 keV, in conflict with a common assumption in appli-
cations of photoelectron spectroscopy; namely, that the dipole approximation
is strictly valid for photon energies below 1 keV. The potential significance
of these findings is nicely illustrated by comparison of the present results [31]
for the Ne β_{2p} parameter with earlier results [25], where the influence of non-
dipole effects was assumed negligible. Large deviations in the measured β_{2p}
parameters are directly attributable to "contamination" of the previous mea-
surements [25] by non-dipole effects. Generalization of this observation to
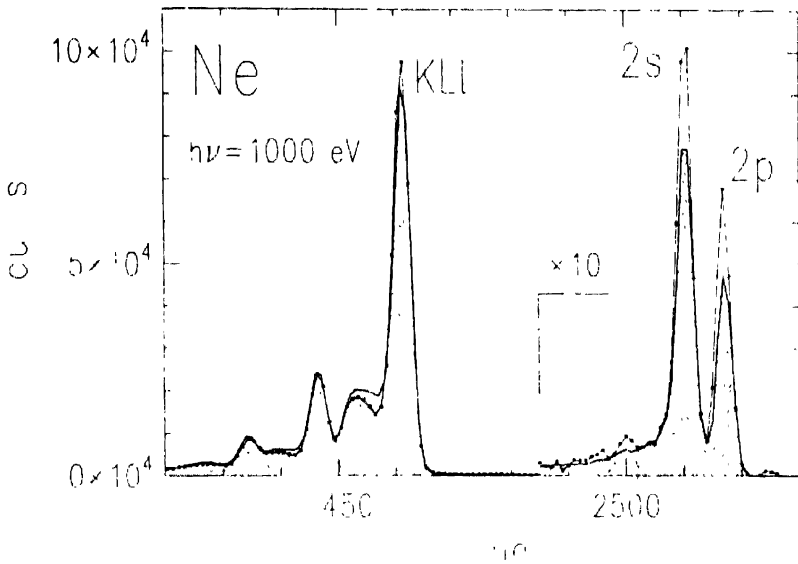
Fig. 2. Photoelectron spectra of Ne measured at a photon energy of 1000 eV. The gray spectrum was taken with the dipole magic-angle analyzer and the other spectrum with the non-dipole magic-angle analyzer. See text for detail.

any angle-resolved photoemission measurement suggests that relative photo-emission peak intensities as a function of angle can be influenced significantly by non-dipole interactions even at photon energies below 1 keV. Therefore, a need for caution in interpreting angle-resolved photoemission data from gases, solids, and surfaces using soft-x-ray excitation is indicated.

These new measurements on neon were performed at the ALS on undulator beamline 8.0 [32], which covers the 100-1500-eV photon-energy range. Because the photon resolution needed to resolve the Ne $2s$ and $2p$ valence lines is low ($E/\Delta E \leq 200$), the monochromator entrance slit was set to 65 μm and the exit slit to 800 μm yielding very high flux. During the measurements the ALS operated at 1.9 GeV in two-bunch mode, giving a photon pulse every 328 ns. The interaction region, formed by an effusive gas jet intersecting the photon beam, has a diameter of about 2 mm. Energy resolution of the TOF analyzers with a focus size of 2 mm is 3% of the electron kinetic energy. Spectrum were collected for about 300 s, with count rates of up to 10^5 s^{-1} in the Ne $2s$ photoline.

From Eq. (1), it is known that photoelectron peak intensities are independent of the β parameter at the so called *magic angle*, θ =54.7°. To take

full advantage of this, the TOF apparatus is designed to simultaneously have one analyzer positioned at $\theta = 0°$ and ϕ i= 90°, a second analyzer at $\theta = 54.7°$ and ϕ i= 90° (referred to as the *dipole magic-angle analyzer*) and a third analyzer at $\theta = 54.7°$ and $\phi = 0°$ (the *non-dipole magic-angle analyzer*). Peak intensities in the dipole magic-angle analyzer, in the $\phi = 90°$ plane (the plane, containing the ϵ-vector, perpendicular to the photon beam direction, see Fig. 1) are independent of the non-dipole parameters γ and δ (see Eq. (2)), as well as the dipole parameter β. The Ne 2s and 2p valence lines were measured over the photon-energy range from 250--1200 eV at five different chamber rotations, yielding a total of 15 spectra, all at different θ and/or ϕ angles, for each photon energy. This set of spectra provide enough information to determine simultaneously the polarization characteristics of the incident beam and the angular-distribution parameters β, γ, and δ. As one example of non-dipole effects in Ne, Fig. 2 shows two superimposed spectra taken at the dipole magic angle and the non-dipole magic angle. The spectra are scaled to the area of the Ne *KLL* Auger lines. Auger lines arising from an intermediate state with an s hole in a closed-shell system like Ne have an isotropic angular distribution ($\beta = \gamma = \delta$), which makes them ideal for calibration [33]. Thus the angular-distribution parameters of the Ne valence peaks are measured relative to known β, γ, and δ parameters. The obvious intensity differences between the Ne 2s and 2p peaks in the two spectra in Fig. 2 are due entirely to non-dipole effects because both spectra are at the magic angle where the β parameter has no influence.

5.   Conclusion   .

In summary, the X-ray Atomic and Molecular Spectroscopy Program at the Advanced Light Source is now operational. In one of its initial experiments, significant electric-quadrupole and magnetic-dipole effects have been observed in valence photoemission from Ne in the 250-1200 eV photon-energy region. These higher-order $E2$ and $M1$ interactions can in principle affect all measurements in the field of angle-resolved photoelectron spectrometry not made in the $\phi = 90°$ plane at photon energies below 1 keV. This includes not only measurements on gas-phase targets, but also surface, adsorbate, and condensed-matter targets as well. We caution that possible non-dipole effects need to be considered when photoemission measurements are conducted outside the $\phi = 90°$ plane, even for $h\nu < 1$ keV.

Acknowledgments

References

[1] The XAMS team includes T. Åberg, N. Berrah, G. S. Brown, R. Carr, J. W. Cooper, B. Crasemann, P. Glans, D. L. Hansen, O. Hemmers, M. O. Krause, P. W. Langhoff, J. C. Levin, D. W. Lindle, S. T. Manson, P. Neill, R. C. C. Perera, R. H. Pratt, J. A. R. Samson, I. A. Sellin, D. A. Shirley, H. Wang, R. Wehlitz, and S. B. Whitfield.

[2] C. J. Sparks, Jr., Phys. Rev. Lett. **33**, 262, (1974).

[3] P. Eisenberger, P. M. Platzman, and H. Winick, Phys. Rev. Lett. **36**, 623 (1976).

[4] W. Eberhardt, G. Kalkoffen, and C. Kunz, Phys. Rev. Lett. **41**, 156 (1978).

[5] G. S. Brown, M. H. Chen, B. Crasemann, and G. E. Ice, Phys. Rev. Lett. **45**, 1937 (1980).

[6] K. Hämäläinen, D. P. Siddons, J. B. Hastings, and L. E. Berman, Phys. Rev. Lett. **67**, 2850 (1991).

[7] Y. Ma, N. Wassdahl, P. Skytt, J. Guo, J. Nordgren, P. D. Johnson, J.-E. Rubensson, T. Böske, W. Eberhardt, and S. D. Kevan, Phys. Rev. Lett. **69**, 2598 (1992).

[8] A. Kivimäki, A. Naves de Brito, S. Aksela, H. Aksela, O.-P. Sairenen, A. Ausmees, S. J. Osborne, L. B. Dantas, and S. Svensson, Phys. Rev. Lett. **71**, 4307 (1993).

[9] M. A. MacDonald, S. H. Southworth, J. C. Levin, A. Henins, R. D. Deslattes, T. LeBrun, Y. Azuma, P. L. Cowan, and B. A. Karlin, Phys. Rev. A **51**, 3598 (1995).

[10] J. L. Dehmer, A. C. Parr, and S. H. Southworth, *Handbook on Synchrotron Radiation*, Vol. 2, edited by G. V. Marr (North-Holland, Amsterdam, 1987).

[11] I. Nenner and J. A. Beswick, *Handbook on Synchrotron Radiation*, Vol. 2, edited by G. V. Marr (North-Holland, Amsterdam, 1987).

[12] B. Krässig, M. Jung, D. S. Gemmell, E. P. Kanter, T. LeBrun, S. H. Southworth, and L. Young, Phys. Rev. Lett. **75**, 4736 (1995).

[13] D. W. Lindle, P. L. Cowan, R. E. LaVilla, T. Jach, R. D. Deslattes, B.

Karlin, J. A. Sheehy, T. J. Gil, and P. W. Langhoff, Phys. Rev. Lett. **60**, 1010 (1988).

[14]   S. T. Manson and J. H. McGuire, Phys Rev. A **51**, 400 (1995), and references therein.

[15]   L. Andersson and J. Burgdörfer, Phys. Rev. A **50**, R2810 (1994).

[16]   K. Hino, P. M. Bergstrom, Jr., and J. H. Macek, Phys. Rev. Lett. **72**, 1620 (1994).

[17]   R. C. C. Perera, G. Jones, and D. W. Lindle, Rev. Sci. Instrum. **66**, 1745 (1995).

[18]   U. Becker, D. Szostak, H. G. Kerkhoff, M. Kupsch, B. Langer, R. Wehlitz, A. Yagishita, and T. Hayaishi, Phys. Rev. A **39**, 3902 (1989).

[19]   H. A. Bethe and E. E. Salpeter, *Quantum Mechanics of One- and Two-Electron Atoms* (Springer-Verlag, Berlin, 1957).

[20]   J. Cooper and R. N. Zare, J. Chem. Phys. **48**, 942 (1968).

[21]   S. T. Manson and D. Dill, in *Electron Spectroscopy: Theory, Techniques, and Applications*, Vol. 2, edited by C. R. Brundle and A. D. Baker (Academic, New York, 1978).

[22]   M. O. Krause, Phys. Rev. **177**, 151 (1969).

[23]   For unpolarized incident light, $\beta/2$ is replaced by $-\beta/4$ in Eq. (1), and θ is measured between the propagation vectors of the photon and the photoelectron. Otherwise, the essential physics is the same.

[24]   J. W. Cooper, Phys. Rev. A **42**, 6942 (1990); **47**, 1841 (1993).

[25]   F. J. Wuilleumier and M. O. Krause, Phys. Rev. A **10**, 242 (1974).

[26]   M. Ya. Amusia and N. A. Cherepkov, *Case Studies in Atomic Physics*, Vol. 5 (North-Holland, Amsterdam, 1975).

[27]   A. Ron, R. H. Pratt, and H. K. Tseng, Chem. Phys. Lett. **47**, 377 (1977); H. K. Tseng, R. H. Pratt, S. Yu, and A. Ron, Phys. Rev. A **17**, 1061 (1978).

[28]   A. Bechler and R. H. Pratt, Phys. Rev. A **39**, 1774 (1989); **42**, 6400 (1990).

[29]   J. H. Scofield, Phys. Rev. A **40**, 3054 (1989); Phys. Scripta **41**, 59 (1990).

[30]   M. Jung, B. Krässig, D. S. Gemmell, E. P. Kanter, T. LeBrun, S. H. Southworth, and L. Young (to be published).

[31]   O. Hemmers, G. Fisher, P. Glans, D. L. Hansen, H. Wang, S. B. Whitfield, D. W. Lindle, R. Wehlitz, J. C. Levin, I. A. Sellin, R. C. C. Perera, E. W. B. Dias, H. S. Chakarborty, P. C. Deshmukh, and S. T. Manson (to be published).

[32]   R. C. C. Perera, Nucl. Instrum. Methods **A319**, 277 (1992).

[33]   S. Flügge, W. Mehlhorn, and V. Schmidt, Phys. Rev. Lett. **29**, 7 (1972).